Bioelectrochemistry 153 (2023) 108498

Contents lists available at ScienceDirect

Bioelectrochemistry

journal homepage: www.journals.elsevier.com/bioelectrochemistry

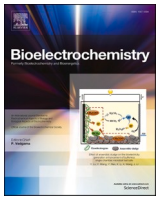

The role of lipid oxidation on electrical properties of planar lipid bilayers and its importance for understanding electroporation

Katja Balantič [a], Victor U. Weiss [b], Ernst Pittenauer [b], Damijan Miklavčič [a], Peter Kramar [a,*]

[a] University of Ljubljana, Faculty of Electrical Engineering, Slovenia
[b] Institute of Chemical Technologies and Analytics, TU Wien, Vienna, Austria

ARTICLE INFO

Keywords:
Lipid oxidation
Planar lipid bilayers
Electroporation
Mass Spectrometry

ABSTRACT

Electroporation is a useful tool for the manipulation with the cell membrane permeability. Underlying physicochemical processes taking place at the molecular level during electroporation are relatively well studied. However, various processes remain unknown, one of them is lipid oxidation, a chain reaction that causes degradation of lipids, and might explain the long-lasting membrane permeability after the electric field has ceased. The aim of our study was to observe the differences in the electrical properties of planar lipid bilayers, as *in vitro* cell membrane models, due to lipid oxidation. Phospholipids were chemically oxidized and oxidation products were analysed using mass spectrometry. Electrical properties, resistance R (Ω) and capacitance C (F) were measured using an LCR meter. Using a previously developed measuring device, a linear increasing signal was applied to a stable bilayer in order to measure its breakdown voltage U_{br} (V) and lifetime t_{br} (μs). We observed an increase in conductance and capacitance of the oxidized planar lipid bilayers when compared to their non-oxidized counterparts. With increasing lipid oxidation, the core of the bilayer becomes more polar, and consequently more permeable. Our findings can explain the long-lasting permeability of the cell membrane after electroporation.

1. Introduction

Electroporation or electropermeabilization is a widely used technique in biotechnology [1,2], medicine [3–5], and food processing [6] for enhancing the permeability of the cell membrane. By application of high-voltage electric pulses, pores are transiently formed in the cell membrane leading to the influx and efflux of various molecules, which otherwise lack the mechanism to cross the hydrophobic membrane barrier [7,8]. However, contrary to results from molecular dynamic (MD) simulations, the membrane's permeability remains high even after the electric field has ceased and the pores have resealed, leading researchers to stipulate that lipid oxidation might contribute to the long-lasting membrane permeability [9–11].

Lipid oxidation is a free radical chain reaction causing the degradation of lipid molecules and is initiated by a radical attack on an acyl chain containing a weak allylic or bis-allylic C–H bond [12]. These double bonds in the fatty acyl chains of unsaturated phospholipids are prone to oxidative damage; in particular to non-specific oxidation caused by reactive oxygen species (ROS). The removal of the hydrogen from the C–H group leaves an unpaired electron on the carbon atom. This creates a carbon-centred lipid radical, which can be stabilized by a shift in double bonds to form a conjugated diene or through the reaction with molecular oxygen to form the lipid peroxide radical [13,14]. Further on, this process creates even more radicals propagating the damage to the nearby molecules since lipid peroxide radicals can abstract hydrogen from a nearby unsaturated lipid molecule, forming a primary oxidation product, hydroperoxide [15]. Oxidative processes can result in various products with truncated lipid tails, as primary products decay further to generate aldehydes as well as carboxylic acids as secondary products [16–18].

Application of high voltage electric pulses could be a stressful event for the cell, leading to oxidative damage of its membrane. Several studies were carried out to confirm that lipid oxidation occurs during electropermeabilization [19], which was indeed shown in bacteria [20], vesicles, liposomes [21] and cells [22–25]. By application of electric pulses, ROS can be generated either in the extracellular medium due to electrochemical reactions or intracellularly due to the destabilization of mitochondrial membranes [25–28]. In a recent MD study it was shown that membrane permeability and conductance increase by several orders of magnitude due to lipid oxidation [11]. In the presence of oxidized

* Corresponding author at: University of Ljubljana, Faculty for Electrical Engineering, Tržaška cesta 25, 1000 Ljubljana, Slovenia.
E-mail address: peter.kramar@fe.uni-lj.si (P. Kramar).

https://doi.org/10.1016/j.bioelechem.2023.108498
Received 25 April 2023; Received in revised form 27 June 2023; Accepted 28 June 2023
Available online 29 June 2023

lipids, the thickness of the bilayer decreases, while the area per lipid increases [29–34], suggesting that, oxidized bilayers are considerably more permeable and conductive than their non-oxidized counterparts [11,35].

Secondary oxidation products were studied as well showing that, due to the formation of aldehydes, the conductance increase is even higher and corresponds to observed conductance changes in cells that were exposed to electric fields [9]. Furthermore, an increase in passive diffusion, as well as spontaneous pore formation can be observed due to increased concentration of oxidized lipids in bilayers. In this context, it was shown that a small number of oxidation products (2.5 %) can already cause a dramatic increase in membrane permeability [36]. It was also observed that membrane oxidation leads to alterations in membrane structure and finally to complete bilayer disintegration [29,37,38]. The extent of lipid oxidation is increased with the number of pulses, pulse duration, and pulse amplitude [22,23,26,39]. Therefore, to further optimize the efficiency of electroporation-based technologies and treatments, in addition to optimizing the electric pulse parameters, we also need to study the relation between the physiological state of the cell membrane, such as its oxidation and its susceptibility to electropermeabilization, to better understand the processes occurring on the molecular level during the application of high voltage electric pulses.

In our study, we measured electrical properties of non-oxidized and chemically oxidized planar lipid bilayers to determine differences due to lipid oxidation. This is a challenging task, which requires characterization of the type and amount of lipid oxidation products. The pathways of oxidative processes vary greatly and depend on the oxidant species, the type of linkage between glycerol and the acyl chain, the degree of unsaturation, and the oxidation conditions. If identification of the oxidation products is relatively simple in lipids with only one bis-allylic hydrogen atom, it becomes more complicated if the degree of unsaturation is increased [12]. Non-oxidized and chemically oxidized lipid molecules with varying degree of unsaturation were analysed by matrix-assisted laser desorption and ionization (MALDI) time-of-flight (TOF) mass spectrometry (MS), which is a simple, but powerful method to characterize lipids and their oxidation products [40,41]. We used different lipid molecules since the unsaturation degree plays a major role in the level of lipid oxidation [21]. We used lipid molecules most commonly studied in MD simulations and as model systems in biomembrane research [9,21,37,42–44].

Planar lipid bilayers as *in vitro* cell membrane models were used to study lipid oxidation processes at the molecular level. This artificial lipid bilayer is an elementary, but still satisfactory model of the cell membrane, used as an electrophysiological technique for measuring the properties of phospholipid molecules, in a controlled environment [45,46]. The composition of the lipid bilayer can be arbitrarily changed to mimic the composition of a true cell membrane with varying degree of oxidized species. With this simple cell membrane model, we were able to thoroughly investigate the electrical properties of lipid membranes that underwent oxidation processes. Electrical properties of non-oxidized or oxidized planar lipid bilayers, such as resistance R (Ω) and capacitance C (F) were measured, and membrane conductance was calculated as an inverse of the measured resistance. A linear increasing signal was applied to a stable bilayer to measure its breakdown voltage U_{br} (V) and the lifetime t_{br} (μs) of the planar lipid bilayer [47,48]. Indeed, we were able to detect measurable differences in the electrical properties of planar lipid bilayers, built from either non-oxidized or oxidized lipid molecules.

2. Material and methods

2.1. Chemicals

N-decane (ReagentPlus, ≥ 99.0 %), hexane (ACS reagent), $KMnO_4$, $FeCl_2$ and H_2O_2 were purchased from Sigma Aldrich (Steinheim, Germany). Chloroform (Spectronorm quality) was obtained from VWR BDH Chemicals (Roncello, Italy), methanol (LiChrosolv), potassium chloride (KCl) and 2-[4-(2-hydroxyethyl)piperazin-1-yl] ethanesulfonic acid (HEPES) from Merck (Darmstadt, Germany). Nitrogen was from Messer (Gumpoldskirchen, Austria). The lipids 1-palmitoyl-2-oleoyl-*glycero*-3-phosphocholine (POPC), 1,2-dioleoyl-*sn-glycero*-3-phosphocholine (DOPC), 1-palmitoyl-2-linoleoyl-*sn-glycero*-3-phosphocholine (PLPC) and 1,2-dilinoleoyl-*sn-glycero*-3-phosphocholine (DLPC) were from Avanti Polar Lipids (Alabaster, AL, USA obtained via Instruchemie (Delfzyl, The Netherlands)). 2′,4′,6′-Trihydroxyacetophenone monohydrate (THAP) matrix substance for MALDI-MS (≥99.5 %) was from Sigma Aldrich (St. Louis, MO, USA).

2.2. Buffers and electrolytes

KCl (0.1 M) and HEPES (0.01 M) were mixed together in a 1:1 volumetric ratio and applied as an aqueous electrolyte in the measurement chamber for planar lipid bilayer measurements.

2.3. Lipid oxidation

All lipids were chemically oxidized prior to bilayer formation using the protocol described in the literature [49]. Briefly, (i) oxidation was carried out with atmospheric air, where lipids in chloroform were dried under a N_2 stream to obtain a dry thin lipid film at the bottom of the flask. Lipids were then left to oxidize under atmospheric air for 1 day. Chloroform was then added, and lipids were used for further experiments. Oxidation was also initiated using either (ii) 2 M $KMnO_4$ solution or a mixture of (iii) 100 mM $FeCl_2$ and 500 mM H_2O_2 solution. Solutions of chemical oxidants were added to the dry thin lipid film at the bottom of the flask and incubated for 10 min at 37 °C using $KMnO_4$ solution or for 1 h using $FeCl_2/H_2O_2$ solution. Afterwards 1 ml of chloroform: methanol [1:1 vol ratio] was added to stop the oxidation. Vortexing and centrifuging were used to separate the polar and non-polar phase and to extract the oxidized lipids, which were dissolved in chloroform and used for further experiments.

2.4. Mass spectrometry analysis

MALDI MS analysis of non-oxidized and chemically oxidized lipids was carried out using an UltrafleXtreme reflectron TOF-MS (Bruker, Bremen, Germany) in positive ion mode at 200 Hz laser repetition rate and accumulating 5000 laser shots per sample. Lipids were dissolved in methanol and pre-mixed (1:1 (v:v)) with methanolic THAP solution (15 mg/ml). 0.6 μl of the final solution was applied to a stainless steel MALDI MS target.

2.5. Planar lipid bilayer formation

Planar lipid bilayers were formed using a Mueller-Rudin method [50,51]. Briefly, the corresponding amount of lipids was dissolved in chloroform and dried under a N_2 stream and subsequently dissolved in *n*-decan to obtain a final 20 mM lipid concentration. Experiments were carried out at room temperature (~21 °C). A Delrin measurement chamber from Warner Instruments (Hamden, CT, USA) with 150 μm diameter aperture separating the two cuvettes was used to form the planar lipid bilayer. The aperture was pretreated with 20 mM lipids dissolved in hexane. After the evaporation of hexane, each compartment was filled with 4 ml of KCl/HEPES electrolyte solution. For planar lipid bilayer formation, a small drop of lipids dissolved in *n*-decane was applied to the aperture using a glass rod. A stable planar lipid bilayer was formed after approximately 30 min and subsequently, capacitance was measured to confirm the stability of the bilayer. In accordance with earlier studies, each experiment was repeated to a minimum of 10 to 20 times to confirm the trend and to avoid errors [52].

This bilayer formation ensures that our lipid molecules are not exposed to air during the formation process. However, due to deposition

of the lipids dissolved in organic solvent directly into the aqueous electrolyte, the solvent itself can play a role in the stability and thickness of the bilayer.

2.6. Planar lipid bilayer resistance and capacitance measurements

Electrical properties of planar lipid bilayers were measured using a system developed in the Laboratory for Biocybernetics, University of Ljubljana, Faculty of Electrical Engineering [48]. The system (Fig. 1) consists of two units that are used for (i) electrical measurements of intact planar lipid bilayers and (ii) to expose the planar lipid bilayer to a linear rising voltage signal.

Electrical measurements on intact planar lipid bilayers were performed using an LCR meter E4980A from Keysight (Santa Rosa, CA, USA) connected to four Ag/AgCl electrodes (In vivo metric, Healdsburg, CA, USA) immersed in the electrolyte solution in the Delrin measurement chamber (Warner Instruments, USA). The LCR meter was set to measure resistance *Rp* and capacitance *Cp* in parallel. The AC voltage was set to 20 mV and the frequency to 2 kHz. Data points were acquired each quarter of a second to obtain measurements of the resistance and capacitance over time.

The breakdown voltage (U_{br}) and lifetime (t_{br}) of the planar lipid bilayer were determined by applying a linear rising voltage signal to a planar lipid bilayer [47]. The signal generator Agilent 33220A, Keysight (Santa Rosa, CA, USA) was used to apply a voltage ramp at 4.8 kV/s. Breakdown voltage was defined as the voltage at the moment t_{br} when a sudden increase of transmembrane current occurred. To detect the current a custom amperometer was developed. Voltage and current signals were measured using an oscilloscope HDO6104A-MS, Teledyne Lecroy (New York, NY, USA). Time of breakdown t_{br} was defined as the lifetime of the lipid bilayer at a chosen slope of the linear rising voltage signal.

A manual switch enables us to differentiate between the two units of the system. The LCR meter, signal generator and oscilloscope were connected through an Ethernet connection and controlled with MATLAB R2019a (MathWorks, Natick, MA, USA) Toolbox using SCPI protocol. Measured capacitance, resistance, breakdown voltage and lifetime of each planar lipid bilayer were processed using MATLAB R2019a.

The specific capacitance c (μF/cm^2) of the planar lipid bilayer was calculated using Eq. (1).

$$c = C_p/A \quad (1)$$

Where C_p is the measured capacitance and A is the area of the aperture (1.76e^{-4} cm^2) used for planar lipid bilayer formation. The electrical conductivity σ (S/cm^2) of the planar lipid bilayer was calculated using Eq. (2) and is the inverse of the measured resistance R_p.

$$\sigma = 1/(R_p{*}A) \quad (2)$$

Specific capacitance and conductance were normalized to the area A of the aperture for easier comparison with the data found in the literature.

To study the effect of lipid peroxidation on the conductivity of planar lipid bilayers, either oxidized or non-oxidized lipids were used. 10 measurements for each lipid species were carried out for each oxidation protocol. Differences in conductance σ and specific capacitance c of the planar lipid bilayers build from either non-oxidized or oxidized lipid molecules were studied.

2.7. Statistical analysis

Resistance and capacitance measurements (N = 10) of planar lipid bilayers for each oxidation procedure and each specific lipid molecule were combined via their mean to obtain the corresponding dataset. Likewise, measurements of the breakdown voltage and bilayer's lifetime (N = 10) for each oxidation procedure and each specific lipid molecule were combined via their mean to obtain the corresponding dataset. Fig. 2 presents raw data. For comparison of planar lipid bilayers datasets, one-way analysis of variance (ANOVA) was used, followed by pairwise comparisons using a multiple comparison Tukey's significant difference procedure. We rejected the null hypothesis of analysis if the p-value of the test was <0.05 ($p < 0.05$). All of the test were performed using Matlab R2019a.

3. Results and discussion

In our experiments, we measured electrical properties of planar lipid bilayers to detect differences between non-oxidized and oxidized bilayers due to lipid oxidation. Bilayer's conductivity, calculated as the

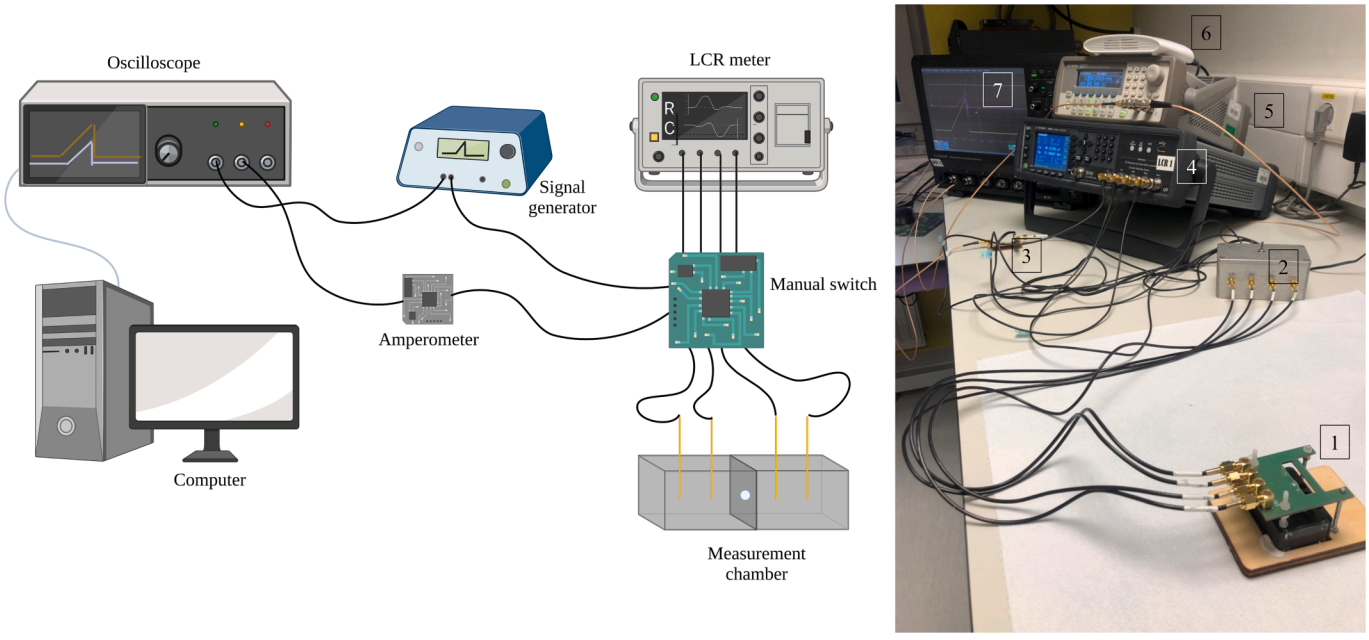

Fig. 1. (Left) A schematics representation of the system developed in the Laboratory of Biocybernetics to measure the electrical properties of planar lipid bilayers. (Right) System in our lab: (1) Measurement chamber, (2) Manual switch, (3) Amperometer, (4) LCR meter, (5) Signal generator, (6) Ethernet Hub, (7) Oscilloscope.

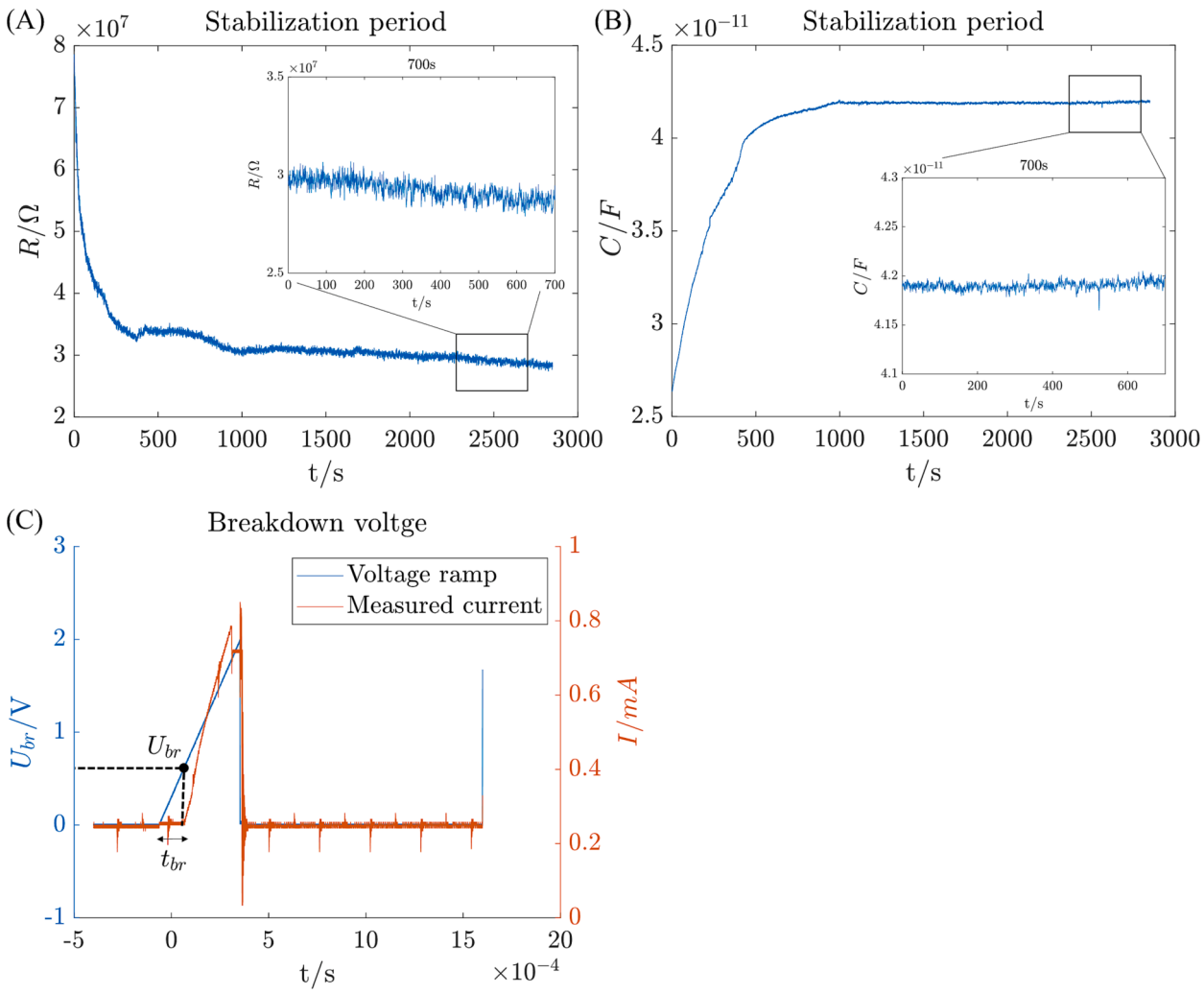

Fig. 2. An example of raw data for a single bilayer measurement. (A) Resistance and (B) capacitance were measured after a minimum of 30 min stabilization period. As the lipids are applied to the aperture in the measurement chamber, the resistance is high and capacitance is low, since a large quantity of lipid molecules is present around the aperture. As the lipids start to self-assemble into a bilayer, the resistance decreases and capacitance increases until both values reach a plateau. When the values of resistance and capacitance were stable, a 700 s measurement of each lipid bilayer was obtained for further analysis. (C) The breakdown voltage U_{br} was measured as the voltage at which the increase in the current was detected. The lifetime t_{br} was measured as the time at which the breakdown of the bilayer occurred.

inverse of the measured resistance, specific capacitance, U_{br} and t_{br} were measured and compared. Oxidation of lipid molecules was carried out using oxidizing agents with varying strength to note different degrees of oxidation. MS analysis was applied to detect produced oxidized species. Below, firstly, the detected oxidation products via MS analysis are described, followed by the analysis of the observed differences in the electrical properties of the planar lipid bilayers due to lipid oxidation.

3.1. Mass spectrometry analysis of lipid molecules

We chemically oxidized the lipids and determined the most common oxidizing products of each specific lipid molecule. The lipid molecules used were: (i) POPC with a single double bond on unsaturated acyl chain at *sn*-2. (ii) DOPC with two double bonds, one each per an acyl chain. (iii) PLPC, which has two double bonds on the unsaturated linoleic acid at *sn*-2. Lastly, (iv) DLPC with four double bonds, 2 each per an acyl chain. The acyl chains differ in the number and the position of double bonds. Since double bonds are highly reactive and play a key role in lipid oxidation reactions, we observed the differences occurring due to variance in double bond number and their position.

3.1.1. Chemistry of lipid oxidation

We used three different oxidation procedures, each one generating radical species with varying strength and, consequently, a different quantity of oxidation products. The most commonly formed oxygen radicals for each oxidation protocol are given below.

The sequential reduction of molecular oxygen (Eq. (3) present in atmospheric air leads to formation of oxygen radicals such as the superoxide anion radical ($O_2^-\bullet$), singlet oxygen ($^1O_2$) and, if H_2O is present, the hydroxyl (HO•) and hydroperoxyl (HOO•) radical [53,54].

$$O_2 + e^- \rightarrow O_2^-\bullet \quad (3)$$

The superoxide radical can further be reduced to form hydrogen peroxide H_2O_2.

$$O_2^-\bullet + e^- + 2H^+ \rightarrow H_2O_2 \quad (4)$$

Furthermore, hydrogen peroxide can further dissociate into the hydroxyl radical (HO•).

$$H_2O_2 + e^- \rightarrow OH^- + HO\bullet \quad (5)$$

Another important ROS is the singlet oxygen, which is formed by the photolysis of the triplet oxygen.

$$^3O_2 \xrightarrow{light} {}^1O_2 \quad (6)$$

Singlet oxygen can react with water vapour in the atmosphere to form hydroxyl radicals. Hydroxyl radicals, being highly reactive can then combine with another O_2 molecule to form a hydroperoxyl radical (HOO•).

$KMnO_4$ is a strong oxidant that does not produce any toxic by-products. Oxidation via $KMnO_4$ was carried out at 37 °C in neutral pH, which leads to the formation of radicals as Mn^{7+} is reduced to form Mn^{4+} (Eq. (7)). Therefore, the permanganate (VII) ion is a strong oxidizing agent.

$$MnO_4^- + 2H_2O + 3e^- \rightarrow MnO_2 + 4OH^- \quad (7)$$

Lastly, oxidation via the Fenton reagents leads to the formation of hydroxyl and hydroperoxyl radicals. Iron Fe^{2+} reacts with H_2O_2 and is oxidized to Fe^{3+} during which a hydroxyl radical (HO•) is formed (Eq. (8). Fe^{3+} can then further react (Eq. (9) with another molecule of H_2O_2 to form hydroperoxyl radical (HOO•).

$$Fe^{2+} + H_2O_2 \rightarrow Fe^{3+} + HO^{\bullet} + OH^- \quad (8)$$

$$Fe^{3+} + H_2O_2 \rightarrow Fe^{2+} + HOO^{\bullet} + H^+ \quad (9)$$

These radicals are powerful, non-selective oxidants. Among the ROS, HO• is the most potent damaging radical which can react with all biological molecules, the most susceptible ones being unsaturated fatty acids.

3.1.2. Produced oxidized species

Non-oxidized lipid molecules used in this study and their most common oxidized counterparts that were also found on MS spectra are presented in Fig. 3. Cleavage of a double bond present on *sn*-2 acyl chain in POPC (Fig. 3A) produced an aldehyde (Fig. 3C) at *m/z* 650.4 and a carboxylic acid (Fig. 3D) at *m/z* 666.4 on the MS spectra (Fig. 4A) resulting from the abstraction of terminal carbon atom at C9. Adducts with H^+, K^+ and Na^+ were detected. For DOPC molecules with two oleic acid chains (Fig. 3E), different oxidation scenarios are possible. It is possible to oxidize the one double bond on *sn*-1 or *sn*-2 acyl chain, which results in an aldehyde (Fig. 3G) found on MS spectra (Fig. 4B) at *m/z* 676.4. Furthermore, with $FeCl_2/H_2O_2$ oxidation, we were able to detect an elimination of the *sn*-2 acyl chain at *m/z* 504.3 (Fig. 3H).

PLPC contains saturated palmitic acid at the *sn*-1 position and unsaturated linoleic acid at the *sn*-2 position (Fig. 3I), where oxidation is expected to take place, so the short-chain products are formed as the result of linoleic acid oxidation. Two double bonds are present on the *sn*-2 chain, the first one at position C9 and the second one at position C12. It

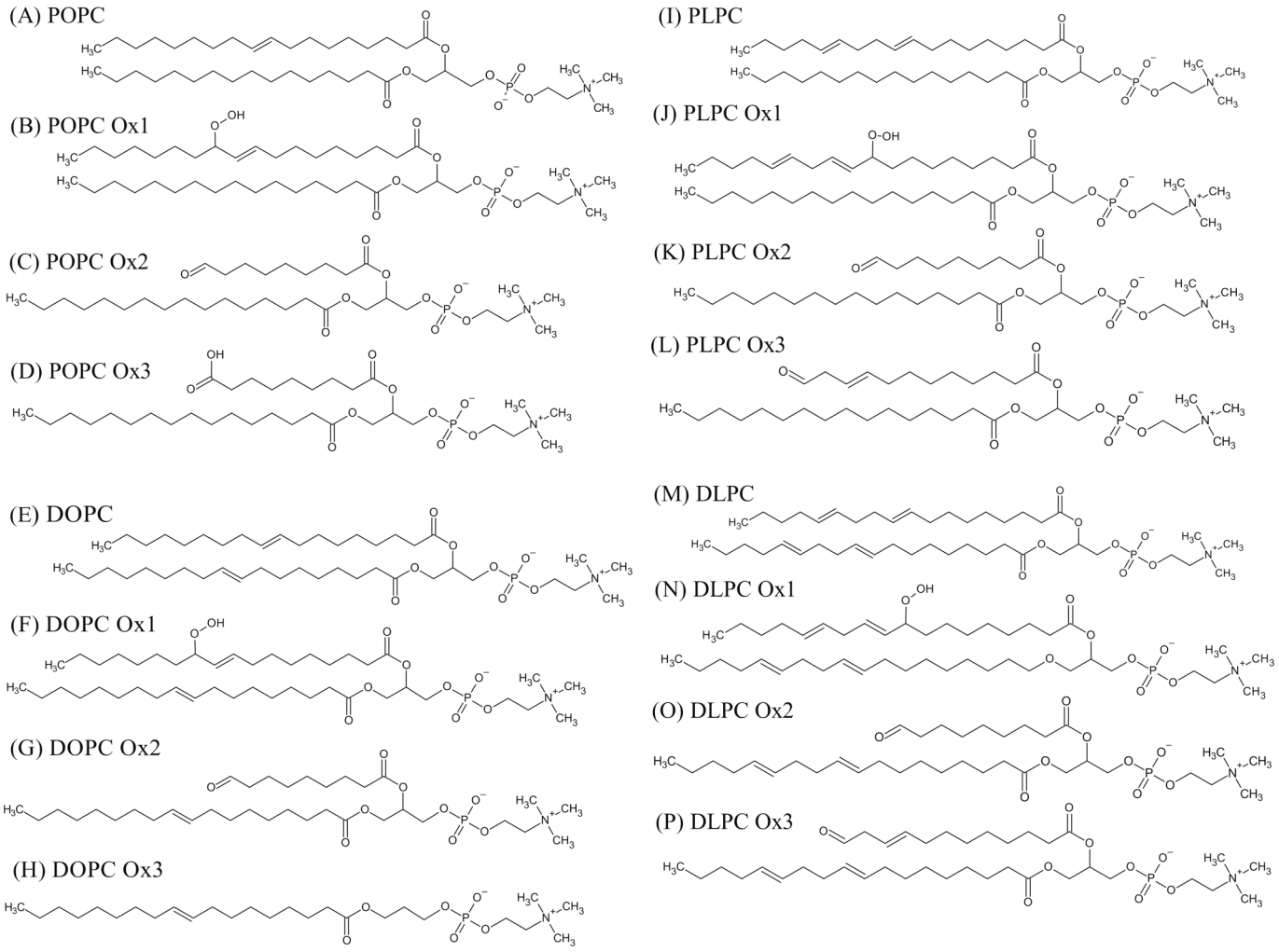

Fig. 3. Non-oxidized lipids used in the study and their oxidized products. (A) Native POPC molecule, (B) hydroperoxide, a primary product of POPC oxidation, (C) oxidation product of POPC with an aldehyde terminal group and (D) oxidation product of POPC with a terminal carboxylic group. (E) Native DOPC molecule, (F) hydroperoxide, a primary product of DOPC oxidation, (G) oxidation product of DOPC with an aldehyde terminal group and (H) elimination of *sn*-2 acyl chain. (I) Native PLPC molecule, (J) hydroperoxide, primary oxidation product of PLPC, (K) oxidation product of PLPC with an aldehyde at position C9 and (L) position C12. (M) Native DLPC molecule, (N) hydroperoxide, primary oxidation product, (O) oxidation product of DLPC with an aldehyde terminal group at C9 and (P) C12.

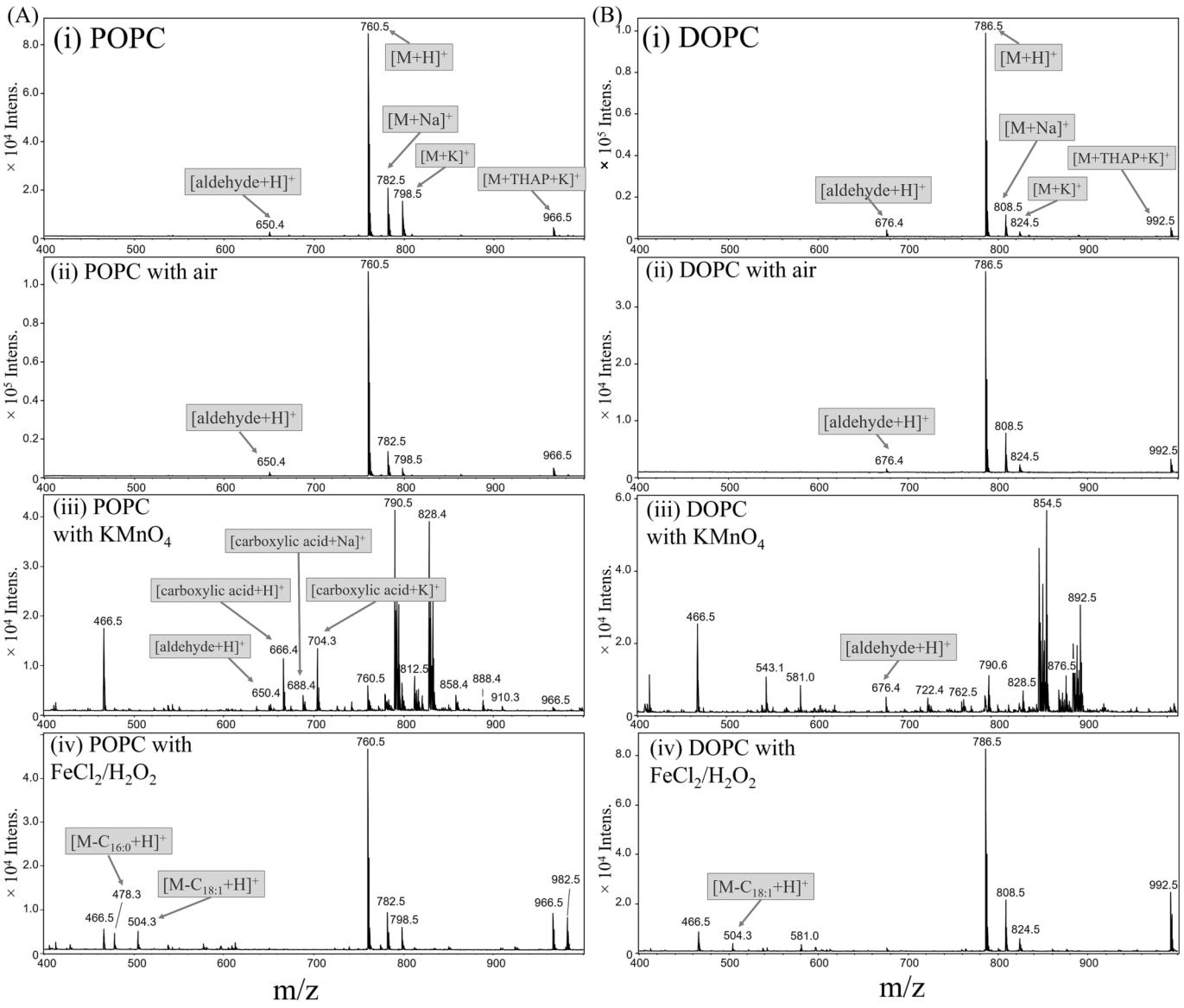

Fig. 4. Mass spectra for (A) POPC, and (B) DOPC lipids. (A) and (B) group on graph include spectra for (i) non-oxidized lipids, (ii) lipids oxidized with air, (iii) $KMnO_4$ and (iv) with Fenton reaction ($FeCl_2/H_2O_2$).

is possible to only oxidize the double bond at position C12 or to shorten the acyl chain even further and oxidize the double bond at position C9. Again mainly aldehydes were found as terminal functional groups due to oxidation, two different aldehydes (Fig. 3K,L) were found, one at C12 with *m/z* 690.4 and one at C9 with *m/z* 650.4 (Fig. 5A). The same is true for DLPC lipid (Fig. 3M) oxidation where the shortenings can occur at two different positions, but this time on each acyl chain. A shorter aldehyde (Fig. 3O) can be detected at *m/z* 674.4 and the longer aldehyde (Fig. 3P) at *m/z* 714.4 (Fig. 5B). Regardless of the position of the double bond, oxidation of an acyl chain usually results in its cleavage and formation of short-chain products of various chain lengths with terminal aldehyde as a functional group (–CHO).

Furthermore, oxidizing agents also influence the formation of oxidation products especially the occurrence of either short or long-chained products. When lipids were oxidized with air, the peaks for oxidation products were low, and only some trace amounts of aldehydes were found for POPC, DOPC and PLPC lipids. In our protocols, air proved to be the weakest oxidizing agent. All of the lipids were dissolved in chloroform and handled in the presence of nitrogen, nevertheless the MS spectra of non-oxidized and air oxidized lipids are not significantly different, leading us to believe that either a trace amount of aldehydes was already present in our native samples, or air does not significantly oxidized the lipids.

$KMnO_4$ oxidation was indeed much stronger than air and resulted in many different products. For POPC lipids, aldehyde as well as carboxylic acid peaks were detected. The peaks for native POPC, DOPC and PLPC molecules are no longer detectable after $KMnO_4$ oxidation since native molecules are cleaved to form the corresponding oxidation products. However, oxidation with $KMnO_4$ produced large peaks even at molecular weights higher than the native lipid molecule, leading us to believe that some of the oxygen remains bound to our lipid molecules even after lipid extraction. This is seen especially on POPC (Fig. 4A) and DOPC spectra (Fig. 4B). The insertion of oxygen atoms without breakdown of the lipid structure generates so-called long-chain products. $FeCl_2$ and H_2O_2 oxidation results in cleavage of a fatty acid from the POPC and DOPC lipid molecule. For PLPC aldehyde was detected, while DLPC is so highly unsaturated that only short-chain products were present, native DLPC molecule was no longer detectable. Several undefined peaks can be found in PLPC (Fig. 5A) and DLPC spectra (Fig. 5B) since they have more possible oxidation scenarios, acyl chains can be cleaved at two

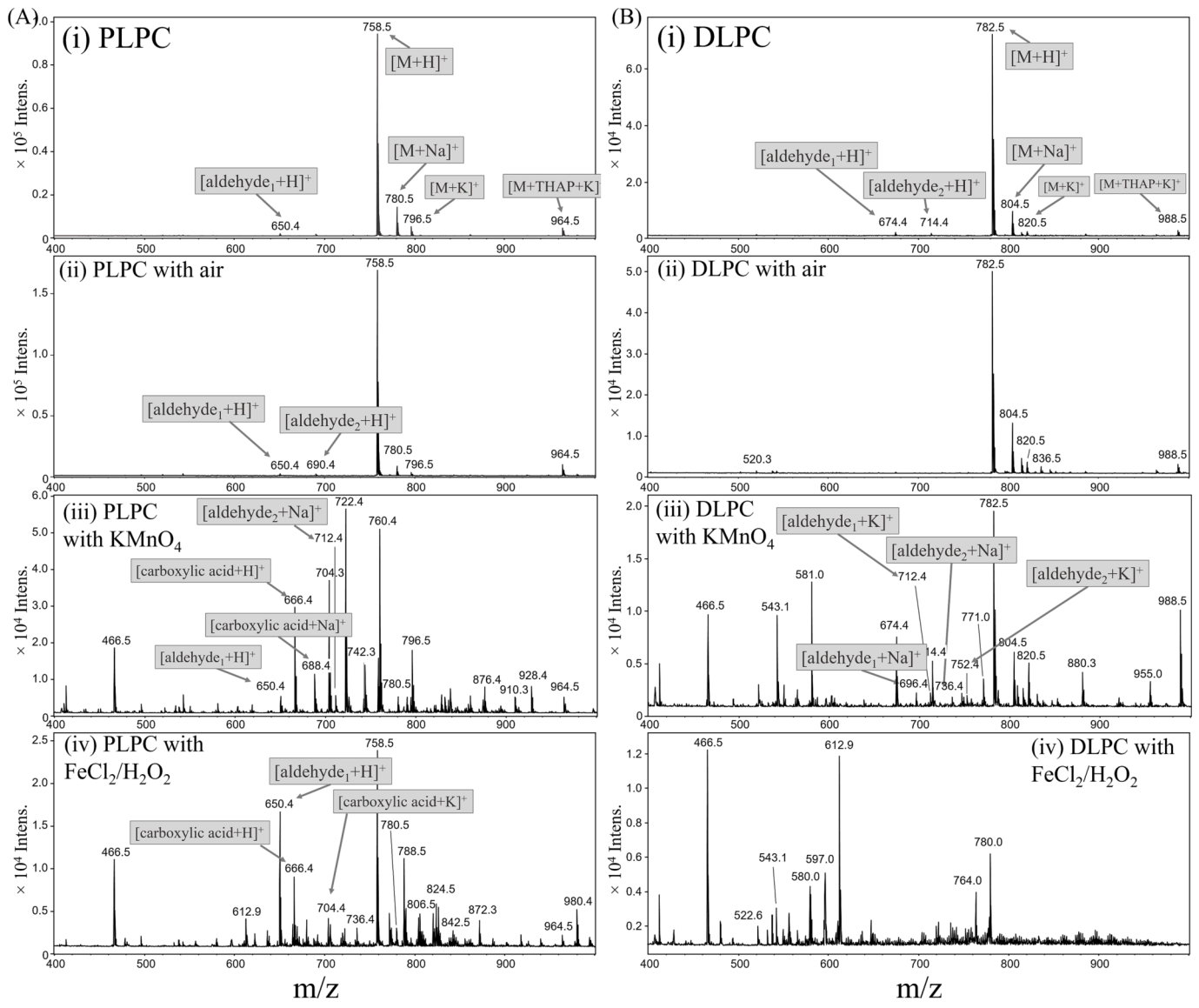

Fig. 5. Mass spectra for (A) PLPC, and (B) DLPC lipids. (A) and (B) group on graph include spectra for (i) non-oxidized lipids, (ii) lipid oxidized with air, (iii) $KMnO_4$ and (iv) with Fenton reaction ($FeCl_2/H_2O_2$).

different positions, and therefore more peaks can be found in the respective MS spectra. Nevertheless, all three oxidation protocols generate similar oxidation products although the yields of the individual compounds are obviously different.

3.2. *Electrical properties of planar lipid bilayers*

Electrical properties of planar lipid bilayers, namely conductivity, specific capacitance, breakdown voltage and lifetime were determined by measuring voltage and current across a planar lipid bilayer. Results show that we are able to detect differences in the electrical properties of non-oxidized and oxidized planar lipid bilayers.

3.2.1. *Conductivity measurements*

A much higher specific conductance of the oxidized planar lipid bilayers, compared to non-oxidized ones, was observed (Fig. 6) indicating that lipid oxidation could be the cause of increased membrane permeability during and after electroporation. The conductivity of the bilayer measures the ability of electrical current and ions to pass the bilayer. With increasing lipid oxidation, the core of the bilayer will become more polar, due to chemical changes and consequently more permeable [55]. Therefore, an increase in conductivity is as expected. Increased conductivity can also affect action potential generation and propagation [56]. What is more, transient pores can occur in the planar lipid bilayer, due to the presence of oxidized species and applied voltage, which could also lead to an increase in specific conductance [57,58]. Our measurement system applies a voltage to the planar lipid bilayer, which could in principle lead to the formation of water fingers that protrude inside the hydrophobic core of the membrane; nevertheless, the bilayer would remain stable. It was shown before, that the presence of oxidized species in the bilayer lowers the activation barrier for pore formation [34]. This gives another possibility for interpretation of an increased specific conductance, not being only due to a decrease in membrane thickness or more hydrophilic bilayer interior, but also because of a lower membrane barrier potential in the presence of oxidized lipid molecules.

Interestingly, as seen in Fig. 6, the conductivity of non-oxidized planar lipid bilayers was the highest for POPC lipids containing a single double bond. This is contrary to expectations since POPC lipids should form the thickest bilayers and therefore have the lowest conductivity. This contradiction can be attributed to the method utilized for bilayer formation. Using the “painting method” for bilayer formation, stable bilayers are readily formed with saturated lipid molecules.

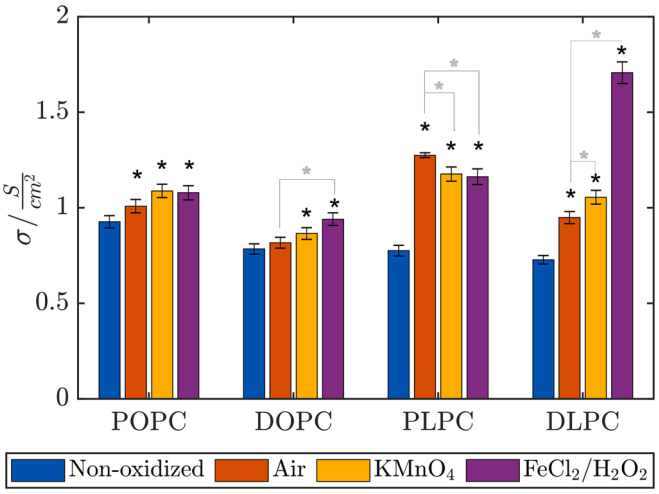

Fig. 6. Specific conductance for each specific lipid bilayer using different oxidation protocols. An increase in membrane conductivity is observed with lipid oxidation. Data are expressed as means ± standard deviations (n = 10 measurements). Black asterisks (*) show statistically significant differences ($p < 0.05$) between non-oxidized and oxidized bilayer, grey asterisks (*) show statistically significant differences ($p < 0.05$) between oxidized groups.

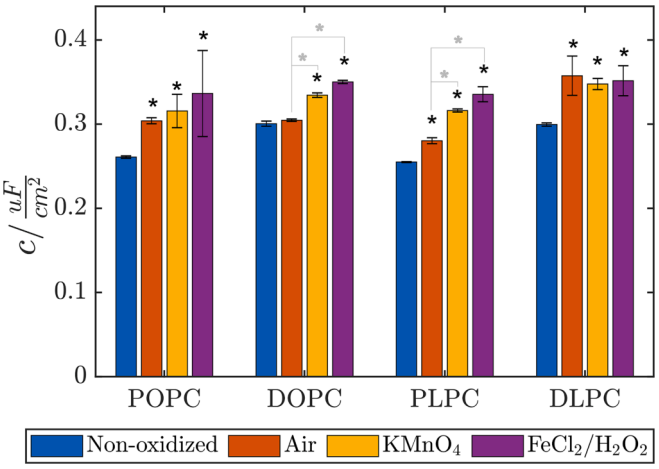

Fig. 7. Specific capacitance for each specific lipid bilayer using different oxidation protocols. Specific capacitance increases due to lipid oxidation. Data are expressed as means ± standard deviations (n = 10 measurements). Black asterisks (*) show statistically significant differences ($p < 0.05$) between non-oxidized and oxidized bilayer, grey asterisks (*) show statistically significant differences ($p < 0.05$) between oxidized groups.

However, when lipids with a higher degree of unsaturation are employed, the bilayers become less stable and their formation requires a larger droplet of lipids to be applied to the aperture in the measurement chamber. Therefore, with higher degree of unsaturation, a larger lipid quantity is needed for bilayer formation, leading to thicker bilayers and possibly to formation of multilayers thus lowering the conductivity for highly unsaturated PLPC and DLPC lipids. The application of multiple droplets to the aperture, could also lead to a higher yield of the solvent within the membrane, consequently thickening the interface and decreasing the conductance. What is more, the nonlinear increase in measured electrical properties for PLPC and DLPC lipids can also be related to a larger degree of lipid unsaturation and presence of various oxidation products. Nevertheless, our aim was to develop a measuring system as a proof of concept to observe differences between non-oxidized and oxidized bilayers for the same lipid species, which was indeed successful for all lipid molecules used.

Conductance of non-oxidized POPC bilayers was 0.92 ± 0.06 S/cm^2. For oxidation with air, the conductance increased for 9 %, while the increase for $KMnO_4$ and $FeCl_2/H_2O_2$ induced oxidation was 16 % and 15 % respectively. DOPC bilayers in their native state had a conductance of 0.79 ± 0.04 S/cm^2. Oxidation with air slightly increased the conductance of the DOPC bilayer for 4 %, while the increase was larger for $KMnO_4$ oxidation with 9 % and a 19 % increase for $FeCl_2/H_2O_2$ oxidation. Non-oxidized PLPC bilayers have a conductance of 0.77 ± 0.05 S/cm^2, their conductance significantly increases with air oxidation, for 65 %. $KMnO_4$ induced oxidation increased the PLPC conductance for 52 % and $FeCl_2/H_2O_2$ for 50 %. DLPC bilayers in the absence of oxidized species have a conductance of 0.73 ± 0.02 S/cm^2. Conductance for oxidation with air and with $KMnO_4$ increased for 28 % and 43 % respectively, while the oxidation via Fenton reagents increased the conductance, more than two-fold, for 134 %, leading us to believe that due to the presence of oxidized species, transient pores form spontaneously and further increase the conductivity of the bilayer.

3.2.2. *Capacitance measurements*

According to our measurements, specific capacitance increased due to lipid oxidation (Fig. 7), which has been reported previously and our results are in agreement with these findings [9]. Oxidation chemically changes the hydrophobic tail region of the lipid molecules, with insertion of more polar functional groups, which increases the dielectric coefficient of the bilayer and consequently results in measureable increase in the lipid bilayer's specific capacitance.

Capacitance of the hydrophobic region is associated not only with the dielectric coefficient but also with the thickness of the phospholipid acyl chains. Oxidation leads to formation of short-chain lipid products, creating thinner bilayers, which results in an increased capacitance.

Specific capacitance of non-oxidized POPC, DOPC, PLPC and DLPC bilayers was 0.26 ± 0.005 μF/cm^2, 0.30 ± 0.01 μF/cm^2, 0.25 ± 0.001 μF/cm^2 and 0.29 ± 0.008 μF/cm^2 respectively. Oxidation of POPC bilayer with air increased the specific capacitance for 15 %, oxidation via $KMnO_4$ for 19 % and with Fenton reagents for 35 %. Specific capacitance of DOPC bilayers increased for 1 %, 10 % and 17 % when lipids were oxidized with air, with $KMnO_4$ or $FeCl_2/H_2O_2$ respectively. Oxidation of PLPC bilayers with air increased the specific capacitance for 12 %, $KMnO_4$ induced oxidation increased the capacitance for 24 %, and the use of Fenton reagents for 32 %. The highest capacitance increase of DLPC bilayers, for 20 % was achieved with oxidation with air; however, the change was not significantly different between other two oxidation protocols. Oxidation with $KMnO_4$ and with $FeCl_2/H_2O_2$ lead to an increase in specific capacitance for 14 % and 19 % respectively.

The value of measured specific capacitance in our study is low compared to previously published reports, which could be due to the incorporation of the hydrocarbon solvent *n*-decane into the membrane [59,60]. What is more, the torus of the solvent surrounding the bilayer could lead to deviations from the previous results as well [61]. Nevertheless, the specific capacitance of the oxidized bilayers increases as seen on Fig. 7, due to the formation of polar regions in previously non-polar environment, and the presence of short-chain oxidation products, which leads to an increase in the bilayer's dielectric coefficient and smaller thickness of the bilayer. However, the differences in specific capacitance, for PLPC and DLPC lipids using the same oxidation protocols are less pronounced than conductivity changes. The fact is that the modifications of the bilayer structure due to the presence of oxidized species are complex. Oxidation induced changes in the acyl chains can also lead to modifications in the head group region of the lipid molecules, where the area per head is increased and functional groups resulting from oxidation are added to the interface [62]. Furthermore, the occurrence of long-chain oxidation products can increase the bilayer thickness. These effects can all lead to smaller specific capacitance differences between non-oxidized bilayers and their oxidized counterparts.

3.2.3. Breakdown voltage and lifetime of planar lipid bilayers

Breakdown voltage and lifetime of planar lipid bilayer are important values when determining the electroporation properties of planar lipid bilayers. Firstly, when applying the voltage ramp, the charge build up on the planar lipid bilayer occurs. Above the critical voltage (U_{br}), defects are caused in the planar lipid bilayer allowing an increase of the transmembrane current, afterwards the bilayers usually collapse [58].

The measured U_{br} (Fig. 8) and t_{br} (Fig. 9) for different bilayers did not prove to be statistically significant, leading us to believe that using our system to obtain the breakdown voltage and lifetime measurements is not a sufficiently sensitive method to detect the differences between non-oxidized and oxidized lipid bilayers. It is interestingly also possible that lipid oxidation does not play a key role in stability of planar lipid bilayers. It was shown recently, that oxidized lipid bilayers can retain their integrity even under applied electric field [34].

We expected that the measurements of breakdown voltage and the lifetime of the oxidized bilayer would show that the voltage needed for the breakdown of the bilayer decreases with lipid oxidation, the same should be true for the bilayer lifetime. The only significant decrease in breakdown voltage and lifetime of the bilayer was obtained for DLPC lipids oxidized with air. DLPC lipids are highly unsaturated and therefore very prone to oxidation. Even though air did not prove to be a strongest oxidant in our experiments, the protocol does not lead to formation of long-chain products. MS spectra for DLPC lipids shows that $KMnO_4$ oxidation leads to formation of aldehydes as well as long-chain products and Fenton reagents lead to no detectable peak for native DLPC molecule, however no known oxidation products were detected either. Therefore, we can only observe a decrease in stability and faster breakdown for DLPC bilayers oxidized with air.

3.3. Lipid oxidation effect on electrical properties of planar lipid bilayer

The study of oxidation effects on different lipid molecules and the measurement of their electrical properties proved to be a challenging task. The bilayer formation becomes more demanding with increasing degree of lipid unsaturation and even more so with the presence of oxidized species. Oxidized bilayers are less stable and a larger quantity of lipid molecules is needed for bilayer formation. Nevertheless, our measurement system enabled us to show, that oxidative stress, and an increasing number of oxidized species perturbing the planar lipid bilayer, leads to an increase in bilayer's conductivity and specific capacitance as summarized in Table 1.

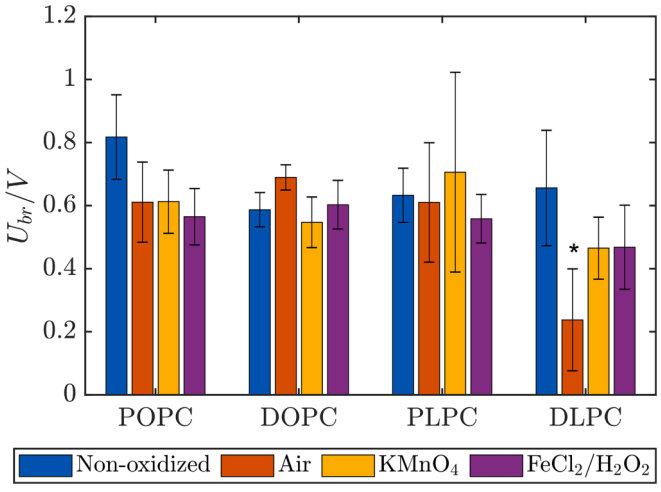

Fig. 8. Breakdown voltage for specific lipid bilayer using different oxidation protocols. A significant decrease in U_{br} was measured for DLPC lipids oxidized in air. Data are expressed as means ± standard deviations (n = 10 measurements). Asterisks (*) show statistically significant differences ($p < 0.05$) between non-oxidized and oxidized bilayer.

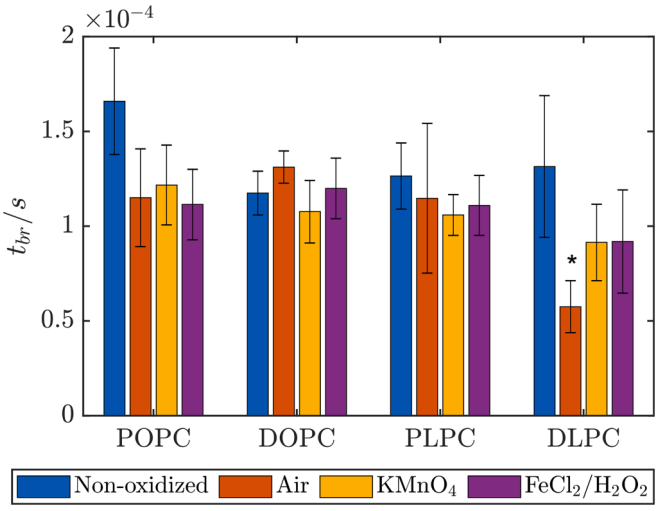

Fig. 9. Lifetime of planar lipid bilayer for specific lipid bilayer and different oxidation protocols. A significant decrease in t_{br} was measured for DLPC lipids oxidized in air. Data are expressed as means ± standard deviations (n = 10 measurements). Asterisks (*) show statistically significant differences ($p < 0.05$) between non-oxidized and oxidized bilayer.

Table 1
Oxidation products and differences in electrical properties for each lipid molecule. –CHO ending corresponds to an aldehyde, –COOH to a carboxylic acid, and M−C16:0, M−C18:1 to fragmentation products. For conductivity and specific capacitance, the mean values with standard deviation are presented. The arrows ↑ indicate an increase in the measured electrical properties for oxidized bilayers compared to their non-oxidized counterparts.

Lipid	Non-oxidized	Air	$KMnO_4$	$FeCl_2/H_2O_2$
POPC	–CHO	–CHO	–CHO, –COOH, less native POPC, long-chain products	Fragmentation: $M-C_{16:0}$, $M-C_{18:1}$
σ (S/cm²)	0.92 ± 0.06	↑ 1.01 ± 0.05	↑ 1.07 ± 0.04	↑ 1.06 ± 0.05↑ 0.35 ± 0.04
c (μF/cm²)	0.26 ± 0.005	↑ 0.30 ± 0.01	↑ 0.31 ± 0.035	↑ 0.35 ± 0.04
DOPC	–CHO	–CHO	–CHO, no native DOPC, long chain products	Fragmentation: $M-C_{18:1}$
σ (S/cm²)	0.79 ± 0.04	↑ 0.82 ± 0.02	↑ 0.86 ± 0.03	↑ 0.94 ± 0.03
c (μF/cm²)	0.30 ± 0.01	↑ 0.303 ± 0.005	↑ 0.33 ± 0.01	↑ 0.35 ± 0.008
PLPC	–CHO	–CHO	–CHO, –COOH, no native PLPC, long-chain products	–CHO, –COOH, long-chain products
σ (S/cm²)	0.77 ± 0.05	↑ 1.27 ± 0.01	↑ 1.17 ± 0.04	↑ 1.16 ± 0.04
c (μF/cm²)	0.25 ± 0.001	↑ 0.28 ± 0.02	↑ 0.31 ± 0.015	↑ 0.33 ± 0.03
DLPC	–CHO	/	–CHO, long-chain products, less native DLPC	Fragmentation, no native DLPC
σ (S/cm²)	0.73 ± 0.02	↑ 0.94 ± 0.03	↑ 1.05 ± 0.04	↑ 1.71 ± 0.05
c (μF/cm²)	0.29 ± 0.008	↑ 0.35 ± 0.035	↑ 0.33 ± 0.025	↑ 0.345 ± 0.03

For POPC lipids, the increase in specific conductance and capacitance is significantly different between non-oxidized and oxidized bilayers (Figs. 6 and 7); however, there is no significant difference between different oxidation protocols. From the POPC MS spectra (Fig. 4A), we were able to observe that air did not produce many oxidation products, while $KMnO_4$ oxidation resulted in high peaks for aldehyde and carboxylic acid products, with H^+, K^+ and Na^+ adducts.

Furthermore, a much smaller peak for native POPC lipid was detectable after $KMnO_4$ oxidation, indicating that the majority of lipids underwent oxidation. Even though high peaks for oxidation products and lower quantity of native POPC were detected on MS spectra, oxidation via $KMnO_4$ did not result in a significant rise in specific conductance and capacitance compared to non-oxidized bilayers. This lack of substantial increase can likely be attributed to the presence of long-chain products as oxygen atoms are incorporated into the acyl chains of the lipid molecules. This long-chain products increase the thickness of the bilayer, minimizing the increase in electrical properties. Oxidation via Fenton reagents led to a decrease in the intensity for native POPC peak and production of two oxidation products due to a removal of either oleic (*m/z* 478.3) or palmitic acid (*m/z* 504.3). However, native POPC lipids were still detectable after $FeCl_2/H_2O_2$ oxidation, and since, bilayers would still preferentially form with non-oxidized native molecules, the increase in specific conductance and capacitance with $FeCl_2/H_2O_2$ oxidation was not as pronounced as expected.

MS spectra of DOPC lipids (Fig. 4B) shows similar results as the one obtained for POPC lipids, due to the similarity in the number and position of the double bond on the oleic acid moiety. $KMnO_4$ oxidation produced mainly aldehyde as an oxidation product, native DOPC was no longer detectable. Long-chain products due to addition of O_2 molecules can be found on the MS spectra for $KMnO_4$ oxidation, leading to much thicker bilayers and less significant differences in electrical properties (Figs. 6 and 7). Oxidation with $FeCl_2/H_2O_2$ did result in a lower intensity of native DOPC peak and elimination of *sn*-2 acyl chain from DOPC molecule (*m/z* 504.3), therefore producing short-chain products, which resulted in the highest increase in specific conductance and capacitance for DOPC bilayers. Oxidation with air did not show statistically significant change between non-oxidized and oxidized bilayers.

When bilayers were built from PLPC lipids, oxidation with air caused a highest increase in membrane conductivity, which is surprising, since MS spectra (Fig. 5A) did not show many oxidation products; what is more, the increase in specific capacitance was not as high as conductivity increase. This led us to believe that not only the bilayer thickness but also the change in the dielectric coefficient due to oxidized lipid tails in the bilayer interior has a significant effect on the specific capacitance for PLPC lipids. With air oxidized PLPC lipids, two aldehydes were detected as well as a high peak for native PLPC lipids. Therefore, a stable bilayer was readily formed with lower lipid quantity, leading to a thinner bilayer with a fraction of integrated aldehydes. Therefore, the conductivity increase was high, while the small presence of oxidized species did cause an increase in the dielectric coefficient, and the difference in specific capacitance between non-oxidized and air oxidized PLPC is not as high. Oxidation with $KMnO_4$ and $FeCl_2/H_2O_2$ produced many oxidation products, mainly aldehydes and carboxylic acids. With $KMnO_4$ oxidation, native PLPC molecule was no longer detectable. However, a less significant increase in PLPC conductance (Fig. 6) was measured for $KMnO_4$ and $FeCl_2/H_2O_2$ oxidation compared to air oxidation. This could be explained by a larger lipid quantity need for formation of a stable PLPC bilayer in the presence of $KMnO_4$ and Fenton reagents, therefore increasing the thickness of the bilayer and lowering the conductivity for $KMnO_4$ and $FeCl_2/H_2O_2$ oxidation. On the other hand, the specific capacitance increase (Fig. 7) was the highest when $FeCl_2/H_2O_2$ was used to oxidized PLPC lipids, probably due to a large increase in dielectric coefficient.

For DLPC the Fenton reagents produced the highest amount of short-chain products, original DLPC was no longer detectable on the MS spectra (Fig. 5B) and consequently the highest increase in membrane conductance (Fig. 6), almost two-fold. The measurements of specific capacitance (Fig. 7) showed that there is no significant change between different oxidation protocols for DLPC lipids. Again, leading us to believe that bilayer thickness as well as dielectric coefficient affects the capacitance measurements. When lipids were oxidized using $KMnO_4$ or $FeCl_2/H_2O_2$, chemicals were introduced to the dry lipid film, therefore an ion or a molecule could be left over from the oxidizing chemicals to bind to the lipid. Particularly the $KMnO_4$ induced oxidation leads to the addition of one or two O_2 molecules. Addition of H_2O_2 may also occur. Consequently, not only short-chain but also long-chain products can be formed, leading to a much thicker bilayer with a lower specific capacitance. What is more, the breakdown voltage and lifetime of planar lipid bilayers decreased for highly unsaturated DLPC lipids oxidized with air, which again suggests that the presence of oxidized lipids renders the bilayer less stable. Among all of the lipid molecules studied, the highest change in the electrical properties, especially conductivity was measured for DLPC lipids, due to their high unsaturation and susceptibility to oxidation.

A drawback of our bilayer formation method is the unknown composition of oxidized bilayers. We cannot determine the degree of oxidized species present in the bilayers, only the detection of oxidation products on MS spectra prior to bilayer formation is possible. However, the results show that we are indeed able to detect differences in the electrical properties of non-oxidized and oxidized planar lipid bilayers. What is more, a so-called "folding method" could be used for bilayer formation, where a lipid droplet is deposited on the surface of the aqueous solution in the measurement chamber and bilayers are formed by rising the levels of the solution. With this method, the solvent effect becomes negligible and stable bilayers are formed faster since lipid monolayers form on the surface of the aqueous solution, prior to the bilayer formation. Furthermore, a smaller quantity of lipids is needed for bilayer formation; therefore, our conductivity results for non-oxidized bilayers might not be contradictory anymore. The down side of this method is that lipid molecules are exposed to air during the formation process, however, since our results show that air is not the strongest oxidant; the presence of oxygen from the atmosphere could be neglected in future experiments.

The results obtained can explain the long-lasting membrane permeability after electroporation. Since application of high voltage electric pulses can lead to oxidation of lipid molecules, the conductivity of the membrane increases, which means that not only hydrophilic pores, but also lipid oxidation plays a role in non-selective transport during and after electroporation. Oxidized lipid molecules have to be enzymatically repaired or replaced in order to maintain membrane structure and function [63], which takes time, and that can explain how the cell membrane permeability can be increased even up to several minutes after the application of electric pulses has ceased [11].

4. Conclusions

In our study, we were able to demonstrate that lipid oxidation leads to an overall increase in the planar lipid bilayer conductivity and specific capacitance, thus showing the possibility of increased membrane permeability due to lipid oxidation. This finding can also explain prolonged membrane permeability after the application of high-voltage electric pulses in the process of electropermeabilization. Once an electric field is applied, lipid membranes are under attack of ROS leading to lipid oxidation. Different functional groups, such as aldehydes, carboxylic acid and other short-chain products can be found in the tail regions of oxidized lipids as shown by mass spectrometry. This may lead to structural and chemical changes of the lipid bilayer, which can alter the membrane properties. We detected increased conductivity and specific capacitance of oxidized lipid bilayers compared to their non-oxidized counterparts which most probably occurs due to formation of polar regions in the previously hydrophobic interior of the bilayer. A significantly higher change in electrical properties was observed for lipids with multiple double bonds, which are more prone to oxidation and result in a variety of different oxidation products. Measurements of breakdown voltage and lifetime of the planar lipid bilayer however did not show significant differences, leading us to believe, that the oxidized bilayers retain their stability even under applied electric field.

CRediT authorship contribution statement

Katja Balantič: Conceptualization, Methodology, Investigation, Writing – original draft, Writing – review & editing. **Victor U. Weiss:** Methodology, Supervision, Writing – original draft, Writing – review & editing. **Ernst Pittenauer:** Methodology, Supervision, Writing – original draft, Writing – review & editing. **Damijan Miklavčič:** Supervision, Writing – original draft, Writing – review & editing. **Peter Kramar:** Conceptualization, Methodology, Supervision, Investigation, Writing – original draft, Writing – review & editing.

Declaration of Competing Interest

The authors declare the following financial interests/personal relationships which may be considered as potential competing interests: [Peter Kramar reports financial support was provided by University of Ljubljana Faculty of Electrical Engineering. Peter Kramar reports a relationship with University of Ljubljana Faculty of Electrical Engineering that includes: employment.].

Data availability

Data will be made available on request.

Acknowledgements

This study was funded by Slovenian Research Agency (ARRS) with grant P2-0249, and Junior Researcher funding to KB. Experiments were partially performed within Infrastructure Program: Network of research infrastructure centres at University of Ljubljana (MRIC UL IP-0510).

References

[1] T. Kotnik, W. Frey, M. Sack, S. Haberl Meglič, M. Peterka, D. Miklavčič, Electroporation-based applications in biotechnology, Trends Biotechnol. 33 (8) (2015) 480–488, https://doi.org/10.1016/j.tibtech.2015.06.002.
[2] C. Rosazza, S. Haberl Meglic, A. Zumbusch, M.-P. Rols, D. Miklavcic, Gene electrotransfer: A mechanistic perspective, Curr. Gene Ther. 16 (2) (2016) 98–129, https://doi.org/10.2174/1566523216666160331130040.
[3] M.L. Yarmush, A. Golberg, G. Serša, T. Kotnik, D. Miklavčič, Electroporation-based technologies for medicine: principles, applications, and challenges, Annu. Rev. Biomed. Eng. 16 (1) (2014) 295–320, https://doi.org/10.1146/annurev-bioeng-071813-104622.
[4] B. Geboers, et al., High-voltage electrical pulses in oncology: irreversible electroporation, electrochemotherapy, gene electrotransfer, electrofusion, and electroimmunotherapy, Radiology 295 (2) (2020) 254–272, https://doi.org/10.1148/radiol.2020192190.
[5] A. Maan, J. Koruth, Pulsed field ablation: A new paradigm for catheter ablation of arrhythmias, Curr. Cardiol. Rep. 24 (2) (2022) 103–108, https://doi.org/10.1007/s11886-021-01630-z.
[6] S. Mahnič-Kalamiza, E. Vorobiev, D. Miklavcic, Electroporation in food processing and biorefinery, J. Membr. Biol. 247 (2014), https://doi.org/10.1007/s00232-014-9737-x.
[7] T. Kotnik, L. Rems, M. Tarek, D. Miklavčič, Membrane electroporation and electropermeabilization: Mechanisms and models, Annu. Rev. Biophys. 48 (1) (May 2019) 63–91, https://doi.org/10.1146/annurev-biophys-052118-115451.
[8] M. Tarek, Membrane electroporation: A molecular dynamics simulation, Biophys. J. 88 (6) (2005) 4045–4053, https://doi.org/10.1529/biophysj.104.050617.
[9] D. Wiczew, N. Szulc, M. Tarek, Molecular dynamics simulations of the effects of lipid oxidation on the permeability of cell membranes, Bioelectrochemistry 141 (2021), 107869, https://doi.org/10.1016/j.bioelechem.2021.107869.
[10] J. Garrec, A. Monari, X. Assfeld, L.M. Mir, M. Tarek, Lipid peroxidation in membranes: The peroxyl radical does not 'Float', J. Phys. Chem. Lett. 5 (10) (2014) 1653–1658, https://doi.org/10.1021/jz500502q.
[11] L. Rems, M. Viano, M.A. Kasimova, D. Miklavčič, M. Tarek, The contribution of lipid peroxidation to membrane permeability in electropermeabilization: A molecular dynamics study, Bioelectrochemistry 125 (2019) 46–57, https://doi.org/10.1016/j.bioelechem.2018.07.018.
[12] A. Reis, C.M. Spickett, Chemistry of phospholipid oxidation, Biochim. Biophys. Acta BBA - Biomembr. 1818 (10) (2012) 2374–2387, https://doi.org/10.1016/j.bbamem.2012.02.002.
[13] E.N. Frankel, Free radical oxidation, in: Lipid Oxidation, Elsevier, 2012, pp. 15–24, doi: 10.1533/9780857097927.15.
[14] H. Yin, L. Xu, N.A. Porter, Free radical lipid peroxidation: mechanisms and analysis, Chem. Rev. 111 (10) (2011) 5944–5972, https://doi.org/10.1021/cr200084z.
[15] E. Niki, Y. Yoshida, Y. Saito, N. Noguchi, Lipid peroxidation: Mechanisms, inhibition, and biological effects, Biochem. Biophys. Res. Commun. 338 (1) (2005) 668–676, https://doi.org/10.1016/j.bbrc.2005.08.072.
[16] I.F.F. Benzie, Lipid peroxidation: A review of causes, consequences, measurement and dietary influences, Int. J. Food Sci. Nutr. 47 (3) (1996) 233–261, https://doi.org/10.3109/09637489609012586.
[17] L.J. Marnett, Lipid peroxidation—DNA damage by malondialdehyde, Mutat. Res. Mol. Mech. Mutagen. 424 (1) (1999) 83–95, https://doi.org/10.1016/S0027-5107(99)00010-X.
[18] K. Uchida, 4-Hydroxy-2-nonenal: a product and mediator of oxidative stress, Prog. Lipid Res. 42 (4) (2003) 318–343, https://doi.org/10.1016/S0163-7827(03)00014-6.
[19] L.C. Benov, P.A. Antonov, S.R. Ribarov, Oxidative damage of the membrane lipids after electroporation, Gen. Physiol. Biophys. 13 (2) (1994) 85–97.
[20] S.-K. Yeo, M.-T. Liong, Effect of electroporation on viability and bioconversion of isoflavones in mannitol-soymilk fermented by lactobacilli and bifidobacteria, J. Sci. Food Agric. 93 (2) (2013) 396–409, https://doi.org/10.1002/jsfa.5775.
[21] M. Breton, L.M. Mir, Investigation of the chemical mechanisms involved in the electropulsation of membranes at the molecular level, Bioelectrochemistry 119 (2018) 76–83, https://doi.org/10.1016/j.bioelechem.2017.09.005.
[22] M. Maccarrone, M.R. Bladergroen, N. Rosato, A.F. Agro, Role of lipid peroxidation in electroporation-induced cell permeability, Biochem. Biophys. Res. Commun. 209 (2) (1995) 417–425, https://doi.org/10.1006/bbrc.1995.1519.
[23] M. Maccarrone, N. Rosato, A.F. Agrò, Electroporation enhances cell membrane peroxidation and luminescence, Biochem. Biophys. Res. Commun. 206 (1) (1995) 238–245, https://doi.org/10.1006/bbrc.1995.1033.
[24] N. Sabri, B. Pelissier, J. Teissie, Electropermeabilization of intact maize cells induces an oxidative stress, Eur. J. Biochem. 238 (3) (1996) 737–743, https://doi.org/10.1111/j.1432-1033.1996.0737w.x.
[25] B. Gabriel, J. Teissie, Generation of reactive-oxygen species induced by electropermeabilization of Chinese hamster ovary cells and their consequence on cell viability, Eur. J. Biochem. 223 (1) (1994) 25–33, https://doi.org/10.1111/j.1432-1033.1994.tb18962.x.
[26] P. Bonnafous, M.-C. Vernhes, J. Teissié, B. Gabriel, The generation of reactive-oxygen species associated with long-lasting pulse-induced electropermeabilisation of mammalian cells is based on a non-destructive alteration of the plasma membrane, Biochim. Biophys. Acta BBA - Biomembr. 1461 (1) (1999) 123–134, https://doi.org/10.1016/S0005-2736(99)00154-6.
[27] V.A. Selivanov, J.A. Zeak, J. Roca, M. Cascante, M. Trucco, T.V. Votyakova, The role of external and matrix pH in mitochondrial reactive oxygen species generation, J. Biol. Chem. 283 (43) (2008) 29292–29300, https://doi.org/10.1074/jbc.M801019200.
[28] O.N. Pakhomova, et al., Oxidative effects of nanosecond pulsed electric field exposure in cells and cell-free media, Arch. Biochem. Biophys. 527 (1) (2012) 55–64, https://doi.org/10.1016/j.abb.2012.08.004.
[29] M. Lis, et al., The effect of lipid oxidation on the water permeability of phospholipids bilayers, Phys. Chem. Chem. Phys. 13 (39) (2011) 17555–17563, https://doi.org/10.1039/C1CP21009B.
[30] G. Weber, et al., Lipid oxidation induces structural changes in biomimetic membranes, Soft Matter 10 (24) (2014) 4241–4247, https://doi.org/10.1039/C3SM52740A.
[31] J. Van der Paal, E.C. Neyts, C.C.W. Verlackt, A. Bogaerts, Effect of lipid peroxidation on membrane permeability of cancer and normal cells subjected to oxidative stress, Chem. Sci. 7 (1) (2016) 489–498, https://doi.org/10.1039/c5sc02311d.
[32] J. Wong-ekkabut, Z. Xu, W. Triampo, I.-M. Tang, D. Peter Tieleman, L. Monticelli, Effect of lipid peroxidation on the properties of lipid bilayers: A molecular dynamics study, Biophys. J. 93 (12) (2007) 4225–4236, https://doi.org/10.1529/biophysj.107.112565.
[33] V. Jarerattanachat, M. Karttunen, J. Wong-ekkabut, Molecular dynamics study of oxidized lipid bilayers in NaCl Solution, J. Phys. Chem. B 117 (28) (2013) 8490–8501, https://doi.org/10.1021/jp4040612.
[34] E.J. Lafarge, P. Muller, A.P. Schroder, E. Zaitseva, J.C. Behrends, C.M. Marques, Activation energy for pore opening in lipid membranes under an electric field, Proc. Natl. Acad. Sci. 120 (11) (2023), https://doi.org/10.1073/pnas.2213112120.
[35] P. Jurkiewicz, et al., Biophysics of lipid bilayers containing oxidatively modified phospholipids: Insights from fluorescence and EPR experiments and from MD simulations, Biochim. Biophys. Acta BBA - Biomembr. 1818 (10) (2012) 2388–2402, https://doi.org/10.1016/j.bbamem.2012.05.020.
[36] K.A. Runas, N. Malmstadt, Low levels of lipid oxidation radically increase the passive permeability of lipid bilayers, Soft Matter 11 (3) (2014) 499–505, https://doi.org/10.1039/C4SM01478B.
[37] L. Cwiklik, P. Jungwirth, Massive oxidation of phospholipid membranes leads to pore creation and bilayer disintegration, Chem. Phys. Lett. 486 (4–6) (2010) 99–103, https://doi.org/10.1016/j.cplett.2010.01.010.
[38] R.P. Mason, M.F. Walter, P.E. Mason, Effect of oxidative stress on membrane structure: Small-angle X-ray diffraction analysis, Free Radic. Biol. Med. 23 (3) (Jan. 1997) 419–425, https://doi.org/10.1016/S0891-5849(97)00101-9.
[39] W. Zhao, R. Yang, Q. Liang, W. Zhang, X. Hua, Y. Tang, Electrochemical reaction and oxidation of lecithin under pulsed electric fields (PEF) processing, J. Agric. Food Chem. 60 (49) (2012) 12204–12209, https://doi.org/10.1021/jf304236h.
[40] B. Fuchs, K. Bresler, J. Schiller, Oxidative changes of lipids monitored by MALDI MS, Chem. Phys. Lipids 164 (8) (2011) 782–795, https://doi.org/10.1016/j.chemphyslip.2011.09.006.

[41] J. Schiller, et al., Matrix-assisted laser desorption and ionization time-of-flight (MALDI-TOF) mass spectrometry in lipid and phospholipid research, Prog. Lipid Res. 43 (5) (2004) 449–488, https://doi.org/10.1016/j.plipres.2004.08.001.
[42] P. Boonnoy, V. Jarerattanachat, M. Karttunen, J. Wong-ekkabut, Bilayer deformation, pores, and micellation induced by oxidized lipids, J. Phys. Chem. Lett. 6 (24) (2015) 4884–4888, https://doi.org/10.1021/acs.jpclett.5b02405.
[43] P.T. Vernier, et al., Electroporating fields target oxidatively damaged areas in the cell membrane, PLoS ONE 4 (11) (2009) e7966.
[44] S. Sankhagowit, S.-H. Wu, R. Biswas, C.T. Riche, M.L. Povinelli, N. Malmstadt, The dynamics of giant unilamellar vesicle oxidation probed by morphological transitions, Biochim. Biophys. Acta BBA - Biomembr. 1838 (10) (2014) 2615–2624, https://doi.org/10.1016/j.bbamem.2014.06.020.
[45] E. Zakharian, Recording of ion channel activity in planar lipid bilayer experiments, Methods Mol. Biol. Clifton NJ 998 (2013) 109–118, https://doi.org/10.1007/978-1-62703-351-0_8.
[46] H.T. Tien, A.L. Ottova, Supported planar lipid bilayers (s-BLMs) as electrochemical biosensors, Electrochimica Acta 43 (23) (1998) 3587–3610, https://doi.org/10.1016/S0013-4686(98)00107-8.
[47] P. Kramar, D. Miklavcic, A.M. Lebar, Determination of the lipid bilayer breakdown voltage by means of linear rising signal, Bioelectrochemistry 70 (1) (2007) 23–27, https://doi.org/10.1016/j.bioelechem.2006.03.022.
[48] P. Kramar, D. Miklavcic, A.M. Lebar, A system for the determination of planar lipid bilayer breakdown voltage and its applications, IEEE Trans. NanoBioscience 8 (2) (2009) 132–138, https://doi.org/10.1109/TNB.2009.2022834.
[49] K. Zschörnig, J. Schiller, A simple method to generate oxidized phosphatidylcholines in amounts close to one milligram, Chem. Phys. Lipids 184 (2014) 30–37, https://doi.org/10.1016/j.chemphyslip.2014.09.003.
[50] P. Mueller, D.O. Rudin, H. Ti Tien, W.C. Wescott, Reconstitution of Cell membrane structure in vitro and its transformation into an excitable system, Nature 194 (4832) (1962), 4832, https://doi.org/10.1038/194979a0.
[51] M. Montal, P. Mueller, Formation of bimolecular membranes from lipid monolayers and a study of their electrical properties, Proc. Natl. Acad. Sci. U. S. A. 69 (12) (1972) 3561–3566.
[52] K. Mallaiya, S. Rameshkumar, S.S. Subramanian, S. Ramalingam, T. Ramachandran, Electrochemical impedance studies on the interaction of midazolam with planar lipid bilayer, Electrochimica Acta 138 (2014) 360–366, https://doi.org/10.1016/j.electacta.2014.06.038.
[53] A. Hellmann, S. Daboss, F. Zink, C. Hartmann, P. Radermacher, C. Kranz, Electrocatalytically modified microelectrodes for the detection of hydrogen peroxide at blood cells from swine with induced trauma, Electrochimica Acta 353 (2020), 136458, https://doi.org/10.1016/j.electacta.2020.136458.
[54] P. Vahalová, M. Cifra, Biological autoluminescence as a perturbance-free method for monitoring oxidation in biosystems, Prog. Biophys. Mol. Biol. 177 (2023) 80–108, https://doi.org/10.1016/j.pbiomolbio.2022.10.009.
[55] N.A. Corvalán, A.F. Caviglia, I. Felsztyna, R. Itri, R. Lascano, Lipid hydroperoxidation effect on the dynamical evolution of the conductance process in bilayer lipid membranes: A condition toward criticality, Langmuir 36 (30) (2020) 8883–8893, https://doi.org/10.1021/acs.langmuir.0c01243.
[56] B. Howard, et al., Characterization of phrenic nerve response to pulsed field ablation, Circ. Arrhythm. Electrophysiol. 15 (6) (2022) e010127.
[57] F. Dehez, L. Delemotte, P. Kramar, D. Miklavčič, M. Tarek, Evidence of conducting hydrophobic nanopores across membranes in response to an electric field, J. Phys. Chem. C 118 (13) (2014) 6752–6757, https://doi.org/10.1021/jp4114865.
[58] P. Kramar, L. Delemotte, A. Maček Lebar, M. Kotulska, M. Tarek, D. Miklavčič, Molecular-level characterization of lipid membrane electroporation using linearly rising current, J. Membr. Biol. 245 (10) (2012) 651–659, https://doi.org/10.1007/s00232-012-9487-6.
[59] O. Purrucker, H. Hillebrandt, K. Adlkofer, M. Tanaka, Deposition of highly resistive lipid bilayer on silicon–silicon dioxide electrode and incorporation of gramicidin studied by ac impedance spectroscopy, Electrochimica Acta 47 (5) (2001) 791–798, https://doi.org/10.1016/S0013-4686(01)00759-9.
[60] J.P. Dilger, S.G.A. McLaughlin, T.J. McIntosh, S.A. Simon, The dielectric constant of phospholipid bilayers and the permeability of membranes to ions, Science 206 (4423) (1979) 1196–1198, https://doi.org/10.1126/science.228394.
[61] S.H. White, Analysis of the Torus Surrounding Planar Lipid Bilayer Membranes, Biophys. J. 12 (4) (Apr. 1972) 432–445, https://doi.org/10.1016/S0006-3495(72)86095-8.
[62] H. Junqueira, et al., Molecular organization in hydroperoxidized POPC bilayers, Biochim. Biophys. Acta BBA - Biomembr. 1863 (10) (2021), 183659, https://doi.org/10.1016/j.bbamem.2021.183659.
[63] G.L. Nicolson, G. Ferreira de Mattos, M. Ash, R. Settineri, P.V. Escribá, Fundamentals of membrane lipid replacement: A natural medicine approach to repairing cellular membranes and reducing fatigue, pain, and other symptoms while restoring function in chronic illnesses and aging, Membranes 11 (12) (2021) 944, https://doi.org/10.3390/membranes11120944.